JACS
JOURNAL OF THE AMERICAN CHEMICAL SOCIETY
Article
pubs.acs.org/JACS

# Generating Long Supramolecular Pathways with a Continuous Density of States by Physically Linking Conjugated Molecules via Their End Groups

Roozbeh Shokri,[†,‡] Marie-Agnés Lacour,[§] Thibaut Jarrosson,[§] Jean-Pierre Lère-Porte,[§] Françoise Serein-Spirau,[§] Karinne Miqueu,[∥] Jean-Marc Sotiropoulos,[∥] François Vonau,[†] Dominique Aubel,[†] Marion Cranney,[†] Günter Reiter,[‡] and Laurent Simon*[,†]

[†]Institut de Sciences des Matériaux de Mulhouse IS2M, LRC 7228-CNRS-UHA, 4 rue des frères Lumière, 68093 Mulhouse, France
[‡]Physikalisches Institut, Universität Freiburg, Hermann-Herder-Strasse 3, 79104 Freiburg, Germany
[§]Institut Charles Gerhardt de Montpellier, UMR 5353-CNRS Equipe Architectures Moleculaires et Matériaux Nanostructurés (AM2N), Ecole Nationale Supérieure de Chimie de Montpellier, 8 Rue de l'Ecole Normale, 34296 Montpellier cedex 05, France
[∥]Institut des Sciences Analytiques et de Physico-Chimie pour l'Environnement et les Matériaux, IPREM, UMR 5254-CNRS, Equipe Chimie-Physique, Université de Pau et des Pays de l'Adour, Hélioparc, 2 Avenue du Président Angot, 64053 Pau Cedex 09, France

**ABSTRACT:** Self-assembly of conjugated 2,5-dialkoxy-phenylene-thienylene-based oligomers on epitaxial monolayer graphene was studied in ultrahigh vacuum by low-temperature scanning tunneling microscopy (STM). The formation of long one-dimensional (1D) supramolecular chain-like structures has been observed, associated to a physical linking of their ends which involved the rotation of the end thiophene rings in order to allow $\pi-\pi$ stacking of these end-groups. d$I$/d$V$ maps taken at an energy corresponding to the excited states showed a continuous electronic density of states, which tentatively suggests that within such molecular chains conjugation of electrons is preserved even across physically linked molecules. Thus, in a self-organization process conjugation may be extended by appropriately adapting conformations of neighboring molecules. Our STM results on such self-organized end-linked molecules potentially represent a direct visualization of J-aggregates.

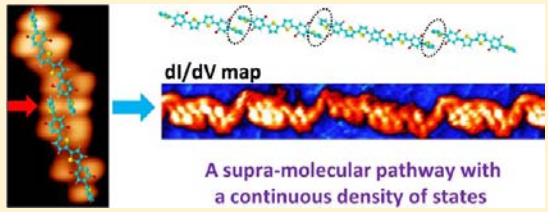


## 1. INTRODUCTION

Numerous research groups have studied possibilities to develop conducting molecular wires.[1−10] The aim is to generate pathways significantly longer than a few molecules which enable coherent electronic transport. Various one-dimensional (1D) self-assembled nanostructures of $\pi$-conjugated molecules have been considered,[11−15] and various molecules without any defects were synthesized.[16−19] Several methods have been successfully employed to obtain long chains of $\pi$-conjugated molecules.[2−4] However, the measured mobility along such chains was often low, most likely due to poor conjugation along the molecular nanostructure. Thus, a major goal is to increase the conjugation length by achieving perfect alignment of the $\pi$-orbitals, for example, of aromatic groups, via a high level of planarity of the molecules which requires rather rigid and planar molecular sequences. Oligo- and polythiophenes, solubilized by attaching alkyl side chains, represent quite suitable model systems.[20] However, deviations from a regioregular arrangement of these side-chains (head-to-tail defects) may decrease the conjugation length and thus degrade transport properties.

Here, we report the formation of supramolecular wires based on oligomers via a specific self-assembly mechanism on graphene. Such physically linked molecules are reminiscent of J-aggregates based on an intermolecular "head-to-tail" coupling restricted to a small part of each molecule.[21−23] The here-studied molecules consist of so-called TBT units, a central dialkoxybenzene core (B), having octyl groups attached laterally and connected to two thiophene rings (T). 2TBT and 3TBT oligomers were used in this study (see Figure 1b). The synthetic approach allowed obtaining perfect regioregularity,[16,18] an essential requirement for generating long supramolecular chains possessing an extended conjugation length.

To study 2D supramolecular organization, we used a monolayer of epitaxial graphene (EG) as asubstrate. In contrast to metal surfaces often used in studies of molecular assembly,[24−27] epitaxial graphene represents a "self-supported", chemically inert layer exhibiting much weaker interactions between molecule and substrate compared to the dominant molecule−molecule interactions. Graphene has been used previously as a substrate which interacts weakly with molecules.[28−30] Graphene and graphite, two substrates with identical chemical composition at the surface, were compared in several previous studies indicating much weaker interactions between molecules and graphene.[28,29,31] Our recent study also

**Received:** December 7, 2012
**Published:** March 22, 2013



dx.doi.org/10.1021/ja311964b | J. Am. Chem. Soc. 2013, 135, 5693−5698

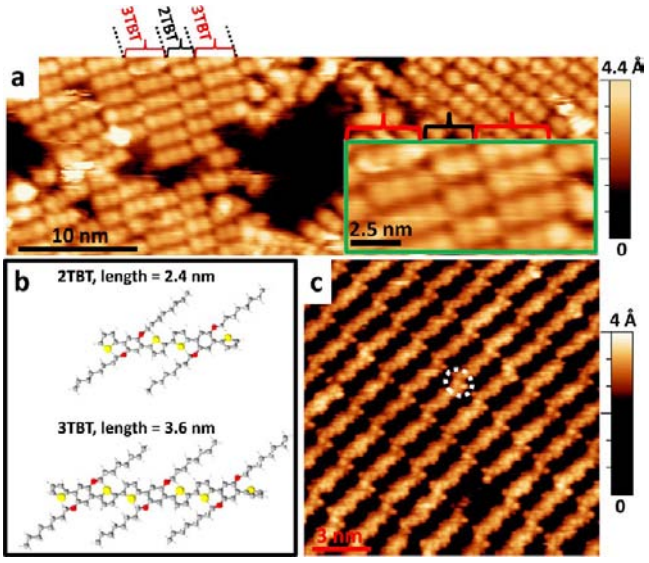


**Figure 1.** (a) STM image (50 × 17 nm$^2$) of 2TBT and 3TBT molecules at positive bias voltage, $V$ = 3.1 V, $I$ = 56 pA, representing an early stage of the assembly process. The inset zooms in on an area composed of rows of 2TBT (black curly bracket) and 3TBT (red curly brackets) molecules. (b) Schematic representation of 2TBT and 3TBT oligomers used in this study (red—oxygen, yellow sulfur, gray—carbon). (c) STM image (15 × 15 nm$^2$) of ordered 2TBT molecules at negative bias voltage, $V$ = −3 V, $I$ = 76 pA. The white dotted ellipse highlights two bright protrusions corresponding to end-thiophene rings physically linking two molecules.

indicates that, although weak, this interaction is sufficient to guide and orient molecules.[31]

## 2. METHODS

**2.1. Experimental Methods.** We have synthesized first TBT molecules as described in ref 17. Then, 3TBT was elaborated by palladium (0) Stille cross coupling between two equivalents of monostannylated TBT moieties and 1 equiv of 2,5′-diiodinated TBT species. 3TBT was isolated as an orange solid with a 30% yield. After flash chromatography purification, the sample may potentially contain 2TBT molecules but at a fraction below the detection limit of $^1$H NMR (400 MHz) spectroscopy. No doublet at 7.45 ppm, typical of 2TBT resonance, was detected in 3TBT $^1$H NMR spectrum (ESI).

The graphene substrates were prepared in ultrahigh vacuum (UHV) by annealing n-doped SiC(0001) for several hours at 900 K followed by annealing at 1500 K.[32,33] The molecules in form of a powder were put in a crucible and heated in UHV. The deposition of molecules on graphene was carried out at a temperature of 500 K corresponding to the first detectable stage of melting as identified by a pressure change to a pressure of ca. $10^{-7}$ mbar in the evaporation chamber. We note that at this temperature the probability of evaporation of traces of 2TBT coexisting in the analytically pure 3TBT sample was significantly higher than for 3TBT molecules. As a result, we deposited and thus observed mostly 2TBT rather than 3TBT molecules on our samples. As an advantageous side effect of evaporating at such low temperature (besides a reduced risk of thermal degradation), we were able to simultaneously deposit and observe 2TBT and 3TBT molecules. Thereby, we also took advantage of fractionation, that is, the formation of separated domains consisting (almost exclusively) of 2TBT or 3TBT.

STM experiments were performed with a LT-STM from Omicron at 77 K at a base pressure in the range of $10^{-11}$ mbar. Bias is applied to the sample. d$I$/d$V$ measurements were performed using standard lock-in techniques by using a modulation voltage of ±20 mV. Both d$I$/d$V$ map and constant current images were acquired simultaneously (see, for example, refs 34 and 35). The reliability of our d$I$/d$V$ maps was confirmed by showing that measurements in constant current yielded to the same results as ones performed in constant height mode. To ensure that the STM tip was clean after several spectroscopy measurements on molecules, control measurements were performed on a bare graphene surface.

**2.2. Computational Methods.** Density functional theory (DFT) calculations were performed with the Gaussian 09 suite of programs,[36] using the hybrid functional B3LYP,[37,38] in combination with the 6-31G(d,p) basis set for all atoms. Except when mentioned otherwise in the text, geometry optimizations were carried out without any symmetry restrictions.

## 3. RESULTS AND DISCUSSION

**3.1. An Unusual Type of Self-Assembly.** Figure 1a shows a typical STM topography image of a small section with submonolayer coverage on EG, representing the deposited molecules in the process of self-assembly. Besides some disordered regions, also well ordered 2D-domains can be seen, consisting of periodic lines of TBT molecules separated by 1.8 nm. This distance corresponds to the length of the lateral octyl side-chains nearly perpendicular to the long-axis of the supramolecular chain (see Figure 1b). Remarkably, the two bright bumps visible at high negative bias voltages (see the example indicated by the dotted ellipse in Figure 1c) suggest an interaction between the end-thiophene rings of the molecules (discussed in more detail later).

**3.2. Spectroscopy Measurements and Molecule–Graphene Interactions.** Figure 2a shows typical d$I$/d$V$ measurements taken at various positions along a 2TBT molecule. The conductance peaks at ca. −1.3 V, −1.6 V,

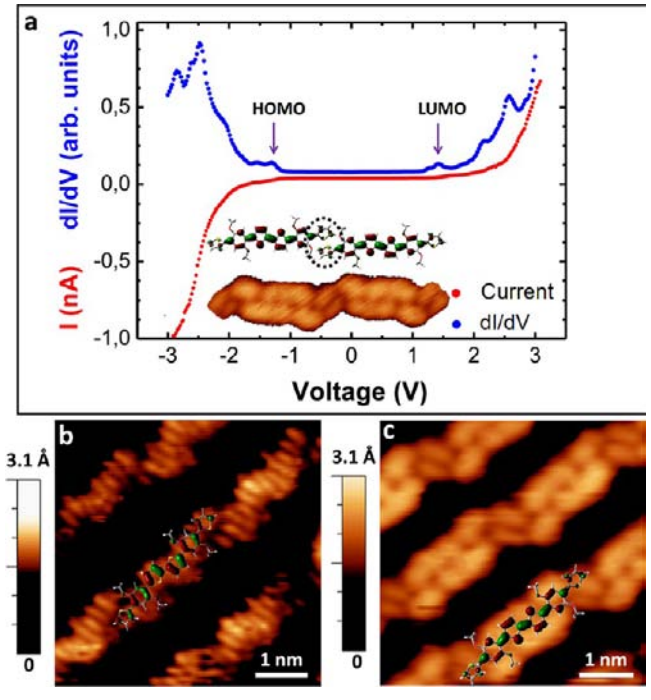


**Figure 2.** (a) $I(V)$ and corresponding d$I$/d$V$ spectroscopy of 2TBT molecules on graphene, measured at various positions along a 2TBT molecule. The inset shows two 2TBT molecules (measured at positive bias voltage) taken from a supramolecular chain. The scheme above the STM image represents the corresponding calculated LUMO orbitals. (b) STM image (4.9 × 4.9 nm$^2$) taken at $V$ = −1.9 V, $I$ = 365 pA. (c) STM image (4.5 × 4.5 nm$^2$) taken at $V$ = +3.1 V and $I$ = 53 pA. The calculated HOMO and LUMO orbitals have been superimposed on the STM images in b and c, respectively.


dx.doi.org/10.1021/ja311964b | J. Am. Chem. Soc. 2013, 135, 5693−5698

−2.15 V, and −2.5 V are attributed to the highest occupied molecular orbitals, HOMO, HOMO-1, HOMO-2, and HOMO-3, respectively. The peaks located at ca. +1.45 V, +2.2 V, and +2.6 V represent the lowest unoccupied molecular orbitals, LUMO, LUMO+1, and LUMO+2. These values result in a HOMO−LUMO gap of 2.75 ± 0.1 eV.

Interestingly, this value is of the same order of magnitude as the value of 2.87 eV obtained through DFT calculations for a free molecule (gas phase) and the measured optical gap of 2TBT in solution (2.56 eV).[39] Besides hinting at a possible electronic coupling between molecules (see later) this value also suggests that the electronic coupling of TBT molecules with EG is weak, i.e., molecular orbitals (MO) are only weakly perturbed by the substrate.[40] Experimentally, similar electronic decoupling was achieved by coating a metallic substrate with a thin insulating layer of NaCl.[41] This is also consistent with recent results of Cho et al.[42] who measured by STS a HOMO−LUMO for $C_{60}$ on EG on SiC(0001) close to the value of solid and gas-phase $C_{60}$. We thus conclude that perfect 2D graphene decouples organic molecules from the semiconducting silicon carbide substrate underneath, in contrast to often used metallic substrates where significant charge transfer is observed. Here, decoupling is also exemplary demonstrated through the submolecular resolution obtained.

**3.3. Submolecular Resolution; Exploring Inter- and Intramolecular Interactions.** Figure 2b and c represents STM topographic images acquired at negative bias voltage $V$ = −1.9 V (probing the occupied states and showing features mostly perpendicular to the molecule axis) and at positive bias voltage $V$ = +3 V (probing the unoccupied states and mostly showing features parallel to the molecule axis), respectively. These STM results are consistent with DFT calculations when integrating the contributions of both HOMO + HOMO-1 (Figure 2b) and LUMO + LUMO+1 + higher MOs (Figure 2c), respectively.

Furthermore, as shown in Figure 3, we were able to resolve MOs for all submolecular parts of the molecules. Each subunit of the molecules could be identified as highlighted in Figure 3a. According to DFT calculations, the comma-like structures shown in Figure 3b are due to large protrusion coming from the oxygen atoms. In Figure 3a and c the two central thiophene rings exhibit the shape of two triangles pointing in opposite directions. Supported by DFT calculations, the apex of the triangle is related to the sulfur atom (Figure 3c). As depicted in Figure 3d, the orientation of thiophene and dialkoxybenzene rings allowed oxygen and sulfur atoms to be in close vicinity. This is a direct evidence of the intrinsic intramolecular, noncovalent sulfur−oxygen (S−O) bridge, expected by DFT calculations,[17] leading to a rigid and planar conformation of the molecule and generating a highly conjugated path along the backbone of TBT molecules.

Our results allow to identify how TBT molecules were connected to each other when forming supramolecular chains within an ordered 2D array. The two bright bumps (labeled by ET in Figure 3i) at both ends of a 3TBT molecule indicate a coupling between molecules by $\pi$-stacking of thiophene rings at the end of these molecules. In contrast, in Figure 3e and f, a single 2TBT was connected to another molecule only in the upper part but not in the lower part. Consequently, only a single bump was visible in the lower part.

Enhancing the contrast as shown in Figure 3f and i helped to identify the other subunits of the molecules at this bias voltage. Interestingly, the molecular orbital can be resolved for HOMO

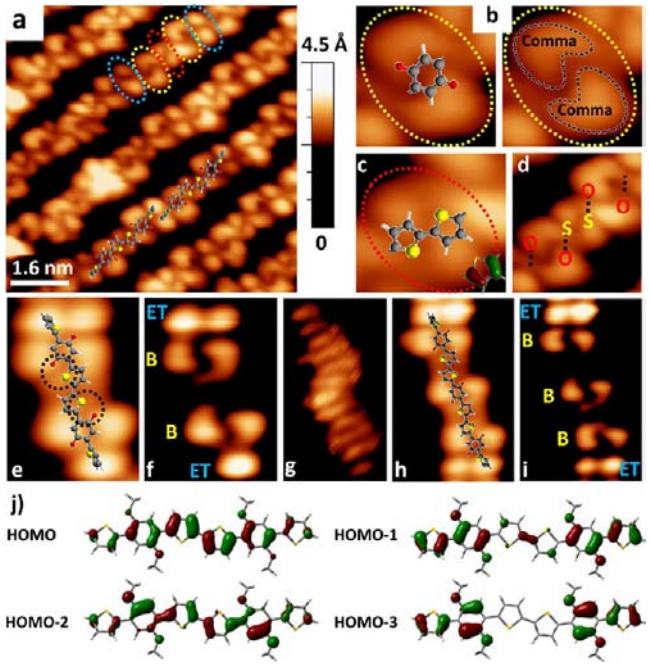


**Figure 3.** Submolecular features in STM images measured at $V$ = −3 V, $I$ = 100 pA (except g: $V$ = −1.9 V, $I$ = 365 pA). (a) Chains of 2TBT or 3TBT molecules. Blue, yellow, and red dotted ellipses mark exemplarily the locations of end thiophene, dialkoxybenzene (see b), and central thiophene rings (see c), respectively. DFT calculation for a central thiophene ring is shown as an inset in c. (d) The close vicinity between the oxygen atom of the dialkoxybenzene segment and the sulfur atom of its first nearest thiophene ring. (e and f) A single 2TBT molecule with one end thiophene (ET) linked to the ET of a neighboring molecule while the other end is free. ETs appear in both cases as bright ellipsoidal protrusions. (h and i) A 3TBT molecule connected at both ends to other molecules in a chain. (f and i) Obtained by changing the visualization contrast of e and h, respectively. (j) Scheme of the calculated molecular orbitals from HOMO level up to HOMO-3 which could contribute to the topographic images at −3 V. In f and i, the end thiophene rings and the dialkoxybenzene groups are labeled by ET and B, respectively. The sizes of the images are: (a) 8 × 8 nm$^2$, (b) 1.1 × 1.1 nm$^2$, (c) 1.1 × 1.2 nm$^2$, (d) 2.1 × 1.9 nm$^2$, (e) + (f) 1.8 × 2.5 nm$^2$, (g) 1.2 × 2.4 nm$^2$, and (h) + (i) 2.2 × 3.5 nm$^2$.

states even in the topographic images (see Figures 3e and f). For a 2TBT molecule measured at $V$ = −1.9 V, exhibiting features in a direction perpendicular to the molecular axis (Figure 3g), a comparison with DFT calculation in j suggests that HOMO and HOMO-1 were integrated. However, for a lower bias voltage (Figure 3f) we observed features parallel to the molecular axis indicating a significant contribution also from lower MOs, that is, HOMO-2 and HOMO-3. This demonstrates that STM measurements on epitaxial graphene on SiC allow to obtain a high submolecular resolution, similar to the situation where the molecule is separated from a metal surface through an insulating layer.[41] However, electrostatic effects may renormalize the HOMO−LUMO gap as pointed out by Neaton et al.[40] and observed also in the case of a metal substrate.[34]

**3.4. Supramolecular Pathway.** The conformation of the octyl chains and possible consequences of connecting molecules via $\pi$-stacking of the end-thiophene-rings are represented by the topographic and the corresponding d$I$/d$V$ images shown in Figure 4a and b, respectively. The central parts


dx.doi.org/10.1021/ja311964b | J. Am. Chem. Soc. 2013, 135, 5693−5698

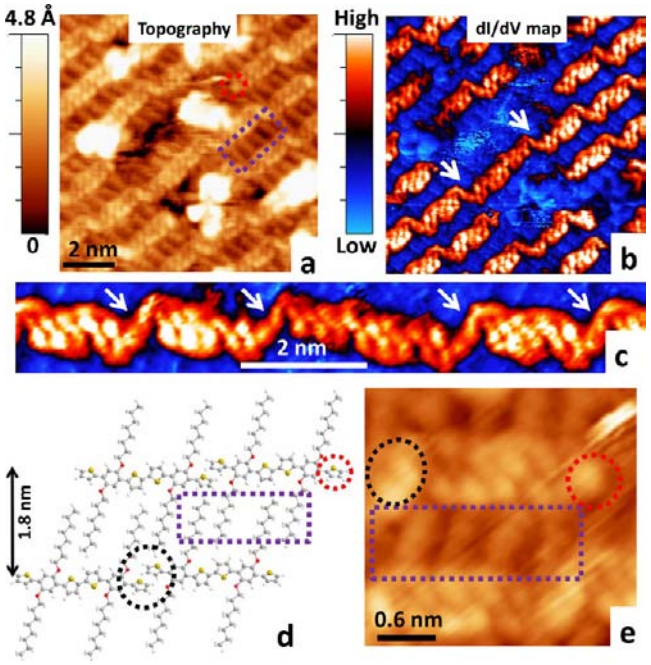


**Figure 4.** (a) Topography STM image ($10 \times 10$ nm$^2$) taken at $V$ = +2.6 V, $I$ = 345 pA, and (b) corresponding d$I$/d$V$ map. (c) The d$I$/d$V$ map of one single chain composed of both 2TBT and 3TBT molecules. (d) Schematic presentation of molecular organization in an ordered 2D lattice of molecules. (e) Two neighboring molecules in two rows of wires. See text for details.

of the molecules as well as the octyl chains were visible. Four such octyl side-chains are highlighted by the dotted rectangle in Figure 4a and e, i.e., two per molecule, clearly exhibiting full interdigitation of octyl chains from neighboring molecules. Consequently, the lateral periodicity perpendicular to the direction of the chains of molecules was ca. 1.8 nm. The angle between octyl side groups and backbone of the molecules was measured to be 82 ± 3°. The lateral octyl side-chains separated the conjugated backbones of the molecules and thus provided a possibility to form insulated molecular wires aligned in a self-assembled supramolecular arrays.

In the cartoon shown in Figure 4d we have assembled the molecules based on the information provided by our STM measurements. For steric reasons, the interacting end-thiophene-rings cannot be both parallel to the substrate. Some rotation is required with respect to the central part of the molecules, which is adsorbed in a planar conformation on the graphene substrate. However, such rotation with respect to the central parts of the molecules potentially prevents that conjugation of an excited state is extended across several molecules. In the d$I$/d$V$ map shown in Figure 4b and c taken at +2.6 V (probing the excited states), we observed a continuity of a bright contrast even across the junctions between two molecules (indicated by white arrows). This continuity of the density of states between molecules provides a support for possible charge delocalization along these chains of molecules. Such a potential increase of the conjugation length from an individual 2TBT molecule to a long connected chain is expected to cause a decrease of the HOMO−LUMO gap. For short molecules with conjugated states along the whole molecule, the molecular resonance energy decreases linearly with length,[43] but eventually approaches an asymptotic value. For the investigated TBT molecules, absorption measurements in solutions of TBT molecules of increasing length showed that the asymptotic value is almost reached already for 4TBT. For 3TBT, 2.39 eV and for 4TBT, 2.33 eV were measured for the energy gap.[39] Thus, from 3TBT to 4TBT, the gap decreased only by 6 meV. Based on these experimental values, the value of the HOMO−LUMO gap for an infinitely long chain of chemically linked and appropriately aligned TBT molecules (expected to have an infinitely long conjugation length) differs only by ca. 230 meV from the value of an individual 2TBT molecule. The continuity in density of states across molecules suggests the possibility of forming J-aggregate-like structures through a physical coupling via their ends. Compared to nonaggregated individual molecules, J-aggregates in solution typically exhibit a red-shift of about 100−200 meV.[21] Recently Yamagata et al.[22] described the engineering of J- and H-aggregates on the basis of wave function overlap. The nature and the vibronic behavior of such aggregates depends on the signs of the electron and hole transfer integrals involving the overlapping LUMO's and HOMO's, respectively, which is very sensitive to the relative stacking (longitudinal and lateral shift) of neighboring conjugated molecules. It seems that self-assembled arrays of TBT molecules enabled us to experimentally influence the design of J (or H) aggregates through controlled overlap of electronic wave functions.

In the here-studied supramolecular chains of TBT molecules, the end-thiophene-rings are separated by a distance of 0.32 ± 0.02 nm (see Figure 5). For such a close stacking distance, DFT calculations suggest a strong overlap of the molecular orbitals, particularly for the excited states. However, overlap, and thus the possibility of having a continuous density of states, decreases rapidly as separation is increased by a few hundredths

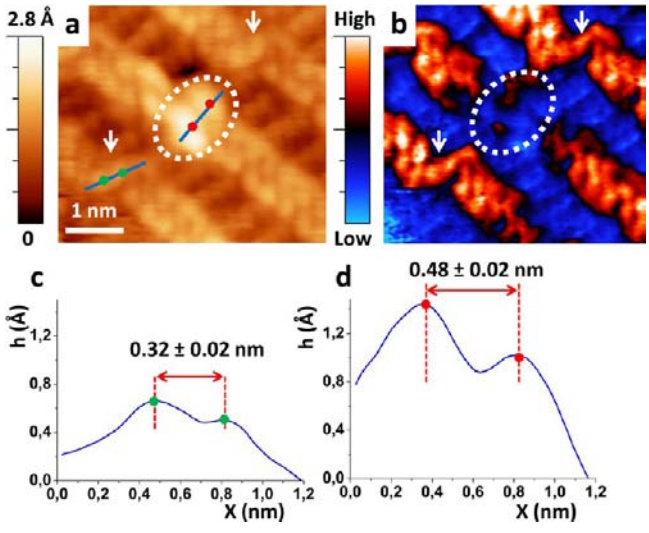


**Figure 5.** (a) Topography STM image ($4.6 \times 4$ nm$^2$) taken at $V$ = +2.6 V, $I$ = 345 pA, and (b) corresponding d$I$/d$V$ map. White arrows in a and b indicate junctions between two molecules exhibiting a continuous density of states. White dotted ellipses encircle the junction between two molecules, where the dihedral angle of end thiophene rings was large and thus caused an interruption in the d$I$/d$V$ map. The pairs of dots highlight the positions of the two end thiophene rings. The distance between the two green dots in a is 0.32 ± 0.02 nm and between the red dots is 0.48 ± 0.02 nm. (c and d) Cross sections along the blue lines in a with green and red dots, respectively.


dx.doi.org/10.1021/ja311964b | J. Am. Chem. Soc. 2013, 135, 5693−5698

of nanometers, as pointed out in a theoretical study on closely packed oligo(phenylene ethynylene) molecules.[44]

It is currently admitted that the conjugation length requires the alignment of aromatic rings within a molecule or along chains of molecules. Wang et al.[43] observed by STM tha,t for a conformational distortion of the torsional angle, causing an increased dihedral angle between adjacent covalently bonded aromatic rings, the density of states showed an interruption at the position of this distortion. Thus, without any specific alignment of aromatic rings between adjacent molecules, one expects that the density of states shows a similar interruption. Nevertheless, our experiments demonstrate that physically linking the end thiophene rings of two adjacent molecules, even when these rings are slightly rotated with respect to the central aromatic rings, a continuous density of states and thus conjugation across molecules can be preserved. DFT calculations suggested that for TBT molecules having a rotation of the end thiophene rings with a dihedral angle up to 45° the conjugation is not significantly disturbed. However, for larger dihedral angles of the end thiophene rings, similar to the experiments of Wang et al.,[43] we observed interruption of density of states at the link between two molecules as clearly shown in Figure 5. The white dotted ellipse in the topography image of Figure 5a identifies two end thiophene rings which are brighter than other end thiophene rings marked by white arrows. The increased brightness observed within the white ellipse is attributed to a larger rotation of the end thiophene rings (compare the height of the peaks in Figure 5c and d). The d$I$/d$V$ map shown in Figure 5b demonstrates that at the position of the two bright protrusions in the topographic image (white ellipse in Figure 5a) the continuity of density of states is broken (white ellipse), while the corresponding two end thiophene are still present at the position of this interruption. Furthermore, the overlap of molecular orbitals and the intermolecular interaction energies between two thiophene rings strongly depend upon their separation distance and their conformation (dihedral angle).[44,45] As shown above, at a junction between two molecules showing a continuous density of states, the end thiophene rings were separated by a distance of 0.32 ± 0.02 nm (this distance was measured at a positive bias voltage). For such close stacking of thiophene rings, DFT calculations suggest a strong overlap of the molecular orbitals, consistent with results by Tsuzuki et al.[45] The latter concluded that the optimum distance between two parallel thiophene rings would be 0.38 nm. In the defect region shown in Figure 5, the apparent distance between the two end thiophene rings (two red dots) is ca. 0.48 nm, which, in turn, results in a weak coupling of these rings, corresponding to the interruption in the d$I$/d$V$ signal (see white dotted ellipse in Figure 5b). Overlap of molecular orbitals, and thus the possibility of having a continuous density of states, decreases rapidly with separation of the rings.

## 4. CONCLUSIONS

In summary, our results suggest that, similar to J-aggregates,[21] long, potentially conductive, supramolecular wires can be formed via a coupling mechanism based on noncovalent bonds. Due to the presence of the octyl side groups and the use of a neutral substrate like epitaxial graphene, these nanowires not only are regularly aligned, but also electrically insulated. The weak interaction between substrate and molecules caused only small perturbations of the electronic structure of the molecules. With the help of DFT calculations, a stabilizing intramolecular, noncovalent interaction (S−O bridge) was identified, which helps improving conjugation. Coupling between molecules was provided by $\pi$-stacking of the thiophene rings at their ends, requiring a certain degree of rotation of these groups with respect to the core of the molecules adsorbed flat on the substrate. Even under such conditions, a strong overlap of all $\pi$-orbitals was evidenced by d$I$/d$V$ map images. The observed continuity of the density of states suggests the possibility of charge delocalization and excitonic energy transport even across the end-groups of these molecules. Dubin et al.[46] demonstrated that isolated polydiacetylene (PDA) chains without any conformational defect, grown in situ from the diacetylene crystal, can act as molecular wires. These authors have observed coherence lengths of excitons of the order of micrometers, that is, excitons being spatially delocalized all along the whole molecules of several micrometers. The fact that we observed a continuous density of states across many TBT molecules hints at the possibility that such chains of noncovalently linked molecules can also represent promising systems for analogous light coherence experiments. Thus, our study provides detailed and spatially resolved insight into the implications of changes of molecular conformation on electronic coupling in the course of a molecular self-assembly process. It suggests an intriguing possibility for generating conductive nanowires by physically linking conjugated molecules which even may allow for coherent charge transport.

## AUTHOR INFORMATION

### Corresponding Author

laurent.simon@uha.fr

### Notes

The authors declare no competing financial interest.

## ACKNOWLEDGMENTS

This work is supported by the Région Alsace and the CNRS, the German Science Foundation (DFG) and the Agence Nationale de la Recherche (ANR) through Grant TRANSFILSEN (ANR-09-BLAN-196).

## REFERENCES

(1) Luo, L.; Choi, S. H.; Frisbie, D. *Chem. Mater.* **2011**, *23*, 631−645.
(2) Tour, J. M. *Acc. Chem. Res.* **2000**, *33*, 791−804 and references therein.
(3) Gonzalez-Rojano, N.; Arias-Marin, E.; Navarro-Rodriguez, D.; Weidner, S. *SynLett* **2005**, *8*, 1259−1262.
(4) Xue, C.; Luo, F. T. *Tetrahedron* **2004**, *60*, 6285.
(5) Sedghi, G.; Garca-Suárez, V. M.; Esdaile, L. J.; Anderson, H. L.; Lambert, C. J.; Martn, S.; Bethell, D.; Higgins, S. J.; Elliott, M.; Bennett, N.; Macdonald, J. E.; Nichols, R. J. *Nat. Nanotechnol.* **2011**, *6*, 517−523.
(6) Nitzan, A.; Ratner, M. A. *Science* **2003**, *300*, 1384−1389.
(7) Choi, S. H.; Kim, B.; Frisbie, D. *Science* **2008**, *320*, 1482−1486.
(8) Cacialli, F.; Wilson, J. S.; Michels, J. J.; Daniel, C.; Silvia, C.; Friend, R. H.; Severin, N.; Samor, P.; Rabe, J. P.; O'Connel, M. J.; Taylor, P. N.; Anderson, H. L. *Nature* **2001**, *1*, 160−164.
(9) Magoga, M.; Joachim, C. *Phys. Rev. B* **1997**, *15*, 4722−4729.
(10) Nozaki, D.; da Rocha, C. G.; Pastawski, H. M.; Cuniberti, G. *Phys. Rev. B* **2012**, *85*, 155327.
(11) Lafferentz, L.; Ample, F.; Yu, H.; Hecht, S.; Joachim, C.; Grill, L. *Science* **2009**, *323*, 1193−1197.
(12) Bombis, C.; Ample, F.; Lafferentz, L.; Yu, H.; Hecht, S.; Joachim, C.; Grill, L. *Angew. Chem., Int. Ed.* **2009**, *48*, 9966−9970.
(13) Kushmerick, J. G.; Holt, D. B.; Pollack, S. K.; Ratner, M. A.; Yang, J. C.; Schull, T. L.; Naciri, J.; Moore, M. H.; Shashidhar, R. *J. Am. Chem. Soc.* **2002**, *124*, 10654−10655.

(14) Repp, J.; Liljeroth, P.; Meyer, G. *Nat. Phys.* **2010**, *6*, 975−979.
(15) Brinkmann, M. *Polym. Phys.* **2011**, *49*, 1218−1233.
(16) Silva, R. A.; Serein-Spirau, F.; Bouachrine, M.; Lère-Porte, J. P.; Moreau, J. J. E. *J. Mater. Chem.* **2004**, *14*, 3043−3050.
(17) Lois, S.; Flores, J. C.; Lère-Porte, J. P.; Serein-Spirau, F.; Moreau, J. J. E.; Sotiropoulos, J. M.; Baylere, P.; Tillard, M.; Bellin, C. *Eur. J. Org. Chem.* **2007**, 4019.
(18) Hermet, P.; Lois-Sierra, S.; Bantignies, J. L; Rols, S.; Sauvajol, J. L.; Serein-Spirau, F.; Lère-Porte, J. P.; Moreau, J. J. E. *J. Phys. Chem. B* **2009**, *113*, 4197−4202.
(19) Kohn, P.; Huettner, S.; Komber, H.; Senkovskyy, V.; Tkachov, R.; Kiriy, A.; Friend, R. H.; Steiner, U.; Huck, W. T. S.; Sommer, J. U.; Sommer, M. *J. Am. Chem. Soc.* **2012**, *134*, 4790−4805.
(20) Bauerle, P.; Fischer, T.; Bidlingmeir, B.; Stabel, A.; Rabe, J. P. *Angew. Chem., Int. Ed. Engl.* **1995**, *14*, 303−307.
(21) Würthner, F.; Kaiser, T. E.; Saha-Möller, C. R. *Angew. Chem., Int. Ed.* **2011**, *50*, 3376−3410.
(22) Yamagata, H.; Pochas, C. M.; Spano, F. C. *J. Phys. Chem. B* **2012**, *116*, 14494.
(23) Spano, F. C. *Acc. Chem. Res.* **2010**, *43*, 429−439.
(24) Vonau, F.; Suhr, D.; Aubel, D.; Bouteiller, L.; Reiter, G.; Simon, L. *Phys. Rev. Lett.* **2005**, *94*, 066103.
(25) Vonau, F.; Aubel, D.; Bouteiller, L.; Reiter, G.; Simon, L. *Phys. Rev. Lett.* **2007**, *99*, 086103.
(26) Yokoyama, T. *Appl. Phys. Lett.* **2010**, *96*, 063101−1.
(27) Bronner, C.; Schulze, G.; Franke, K. J.; Pascual, J. I.; Tegeder, P. *J. Phys.: Condens, Matter* **2011**, *23*, 484005.
(28) Wang, Q. H.; Hersam, M. C. *Nat. Chem.* **2009**, *1*, 206−211.
(29) Huang, H.; Chen, S.; Gao, X.; Chen, W.; Wee, A. T. S. *ACS Nano* **2009**, *3*, 3431−3436.
(30) Zhou, H. T.; Mao, J. H.; Li, G.; Wang, Y. L.; Feng, X. L.; Du, S. X.; Mullen, K.; Gao, H. J. *Appl. Phys. Lett.* **2011**, *99*, 153101.
(31) Shokri, R.; Vonau, F.; Cranney, M.; Aubel, D.; Narladkar, A.; Isare, B.; Bouteiller, L.; Simon, L.; Reiter, G. *J. Phys. Chem. C* **2012**, *116*, 21594−21600.
(32) Simon, L.; Bischoff, J. L.; Kubler, L. *Phys. Rev. B* **1999**, *60*, 11653.
(33) Berger, C.; Song, Z.; Li, T.; Li, X.; Ogbazghi, A. Y.; Feng, R.; Dai, Z.; Marchenkov, A. N.; Conrad, E. H.; First, P. N.; de Heer, W. A. *J. Phys. Chem. B* **2004**, *108*, 19912.
(34) Soe, W. H.; Manzano, C.; Sarkar, A. D.; Chandrasekhar, N.; Joachim, C. *Phys. Rev. Lett.* **2009**, *102*, 176102.
(35) Wang, Y.; Kröger, J.; Berndt, R.; Hofer, W. A. *J. Am. Chem. Soc.* **2009**, *131*, 3639.
(36) Frisch, M. J.; Trucks, G. W.; Schlegel, H. B.; Scuseria, G. E.; Robb, M. A.; Cheeseman, J. R.; Scalmani, G.; Barone, V.; Mennucci, B.; Petersson, G. A.; et al. *Gaussian 09*, Revision A.02; Gaussian Inc.: Wallingford, CT, 2009.
(37) Parr, R. G.; Yang, W. *Density Functional Theory of Atoms and Molecules*, 1st ed.; Oxford University Press: New York, 1989.
(38) (a) Becke, A. D. *Phys. Rev. A* **1988**, *38*, 3098−3100. (b) Becke, A. D. *J. Chem. Phys.* **1993**, *98*, 5648−5652. (c) Lee, C.; Yang, W.; Parr, R. G. *Phys. Rev. B* **1988**, *37*, 785−789.
(39) Narayanan Nair, M.; Hobeika, N.; Malval, J. P.; Alose, S.; Spangenberg, A.; Simon, L.; Cranney, M.; Vonau, F.; Aubel, D.; Serein-Spirau, F.; Lère-Porte, J. P.; Lacour, M. A.; Jarrosson, T., submitted.
(40) Neaton, J. B.; Hybertsen, M. S.; Louie, S. G. *Phys. Rev. Lett.* **2006**, *97*, 216405.
(41) Repp, J.; Meyer, G.; Stojković, S. M.; Gourdon, A.; Joachim, C. *Phys. Rev. Lett.* **2005**, *94*, 026803.
(42) Cho, J.; Smerdon, J.; Gao, L.; Süzer, O.; Guest, J. R.; Guisinger, N. P. *Nano Lett.* **2012**, *12*, 3018−3024.
(43) Wang, S.; Wang, W.; Lin, N. *Phys. Rev. Lett.* **2011**, *106*, 206803.
(44) Jagtap, S. P.; Mukhopadhyay, S.; Coropceanu, V.; Brizius, G. L.; Brédas, J. L.; Collard, D. M. *J. Am. Chem. Soc.* **2012**, *134*, 7176−7185.
(45) Tsuzuki, S.; Honda, K.; Azumi, R. *J. Am. Chem. Soc.* **2002**, *124*, 12200−12209.
(46) Dubin, F.; Melet, R.; Barisien, T.; Grousson, R.; Legrand, L.; Schott, M.; Voliotist, V. *Nat. Phys.* **2006**, *2*, 32.